applied sciences

MDPI

Article

Monitoring Equipment Malfunctions in Composite Material Machining: Acoustic Emission-Based Approach for Abrasive Waterjet Cutting

Ioan Alexandru Popan *, Cosmin Cosma, Alina Ioana Popan, Vlad I. Bocăneț and Nicolae Bâlc

Department of Manufacturing Engineering, Technical University of Cluj-Napoca, B-dul. Muncii, No. 103-105, 400641 Cluj-Napoca, Romania; cosmin.cosma@tcm.utcluj.ro (C.C.); alina.luca@tcm.utcluj.ro (A.I.P.); vlad.bocanet@tcm.utcluj.ro (V.I.B.); nicolae.balc@tcm.utcluj.ro (N.B.)

* Correspondence: ioan.popan@tcm.utcluj.ro

Abstract: This paper introduces an Acoustic Emission (AE)-based monitoring method designed for supervising the Abrasive Waterjet Cutting (AWJC) process, with a specific focus on the precision cutting of Carbon Fiber-Reinforced Polymer (CFRP). In industries dealing with complex CFRP components, like the aerospace, automotive, or medical sectors, preventing cutting system malfunctions is very important. This proposed monitoring method addresses issues such as reductions or interruptions in the abrasive flow rate, the clogging of the cutting head with abrasive particles, the wear of cutting system components, and drops in the water pressure. Mathematical regression models were developed to predict the root mean square of the AE signal. The signal characteristics are determined, considering key cutting parameters like the water pressure, abrasive mass flow rate, feed rate, and material thickness. Monitoring is conducted at both the cutting head and on the CFRP workpiece. The efficacy of the proposed monitoring method was validated through experimental tests, confirming its utility in maintaining precision and operational integrity in AWJC processes applied to CFRP materials. Integrating the proposed monitoring technique within the framework of digitalization and Industry 4.0/5.0 establishes the basis for advanced technologies such as Sensor Integration, Data Analytics and AI, Digital Twin Technology, Cloud and Edge Computing, MES and ERP Integration, and Human-Machine Interface. This integration enhances operational efficiency, quality control, and predictive maintenance in the AWJC process.

Keywords: acoustic emission (AE); composite material; carbon fiber-reinforced polymer (CFRP); monitoring; abrasive waterjet cutting; trimming; industry 4.0; smart manufacturing; digitalization; sensor integration; data analytics

check for updates

Citation: Popan, I.A.; Cosma, C.; Popan, A.I.; Bocăneț, V.I.; Bâlc, N. Monitoring Equipment Malfunctions in Composite Material Machining: Acoustic Emission-Based Approach for Abrasive Waterjet Cutting. *Appl. Sci.* **2024**, *14*, 4901. https://doi.org/10.3390/app14114901

Academic Editors: Slavko Rakic, Ugljesa Marjanovic and Nenad Medic

Received: 9 May 2024
Revised: 29 May 2024
Accepted: 31 May 2024
Published: 5 June 2024

1. Introduction

One advanced composite material that stands out because of its innovative nature is Carbon Fiber-Reinforced Polymer (CFRP). It combines lightweight properties with a unique strength and versatility [1]. CFRP is a versatile material with key characteristics that redefine its applications across industries [2]. This material's adaptability and reliability continue to fuel advancements across the aerospace, automotive, construction, and medical domains [3,4]. Its strength-to-weight ratio is superior to that of traditional materials, making it applicable in the aerospace industry, where lightweight components like wings and fuselage sections contribute to fuel efficiency [5]. CFRP's influence extends to the automotive sector, transforming vehicle design by reducing the weight of body panels and chassis components, thereby enhancing fuel efficiency and maneuverability [6]. In civil engineering, CFRP reinforces structures, ensuring resilience against environmental factors in bridges and buildings [7]. In the medical field, CFRP is used in advanced prosthetics and orthopedic devices, where its strength combines with its lightweight properties for optimal patient comfort [8].

Due to the abrasive wear caused by carbon fibers on cutting tools, CFRP composites are commonly regarded as difficult-to-cut materials [9]. Using inappropriate technologies for machining CFRPs often leads to the emergence of composite-specific geometric defects [10]. These defects may include machining-induced delamination, burrs, fiber fragmentation, fiber pull-out, matrix degradation (such as cracking, smearing, and burning), and fiber–matrix debonding [3,9,10]. The careful selection of technology is important in CFRP manufacturing to prevent the necessity of costly and time-consuming post-machining procedures or component rejection [11].

Abrasive Waterjet Cutting (AWJC) is a machining technique employing a high-pressure stream of water infused with abrasive particles to cut through diverse materials [12]. The process involves pressurizing water, propelling it through a small orifice to form a high-speed jet. The introduction of abrasive particles, such as garnet or aluminum oxide, into the jet stream increases its cutting capacity (Figure 1a). Directed onto the material, the Abrasive Waterjet (AWJ) erodes the substrate, facilitating the creation of complex and precise shapes [5,13]. The following main geometrical kerf characteristics are presented in Figure 1b: the width, taper, and top radius. The AWJ cut surface is categorized into three zones: the initial damage zone (IDZ), the smooth cutting zone (SCZ), and the rough cutting zone (RCZ) (Figure 1c) [10]. AWJC can be used to cut metals, composites, ceramics, and stone [14].

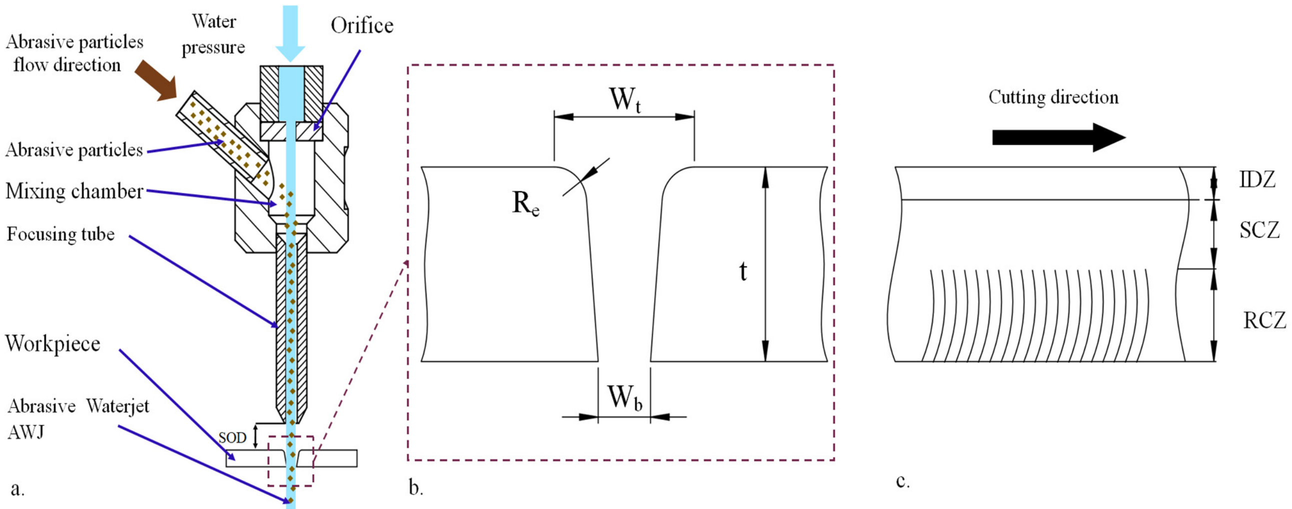

Figure 1. The AWJC principal and kerf characteristics: (**a**) the AWJC principle, (**b**) the kerf geometry, and (**c**) the cut surface characteristics.

AWJ processing offers several advantages over traditional methods like milling or laser cutting for CRFP machining. One of the most significant benefits is that it is a non-thermal process, which eliminates the formation of heat-affected zones and minimizes the risk of thermal distortion or material degradation [10,11]. One of the main damage mechanisms in high-temperature applications is the thermal degradation of the polymer matrix, leading to the deterioration of mechanical properties and the formation of porosities [15]. These porosities can significantly affect the post-processing structural integrity of both the composite material and composite/metal joints by causing delamination [10,15].

Cost-effectiveness is another key advantage of AWJ processing. It often provides low prices with shorter processing times due to its high cutting speed and ability to handle a variety of materials without the need for tool changes or extensive setup adjustments. This efficiency translates into lower operational costs and an increased throughput, making it an attractive option for both small-scale and large-scale manufacturing operations [5,10,16].

Furthermore, it is highly versatile and accurate, capable of accommodating complex geometries with superior dimensional precision (up to ±0.01 mm) and surface quality (up to Ra 0.2 μm) [9,17].

AWJ is used for machining a lot of different parts and components in the aerospace and automotive industries. AWJ cutting is the ideal tool for trimming (external counter cutting) complex parts made from CM. For example, in the case of the Airbus 350 and Boeing 787, the composite stringers used for the T-Beam and I-Beam stiffeners are trimmed using AWJ [16], and different body components of the BMW i3 are machined using AWJ. Machining with AWJ is used in the manufacturing of various products including medical devices, sporting goods, marine components, or wind turbine blades [18].

Machining composite materials with AWJ can lead to various defects, including delamination (cracking) [19], fiber pull-out, abrasive embedment [5], poor surface quality, or low accuracy [10]. The material delamination resulting from the shock created by the high-velocity water jet hitting the material is a significant problem in machining with AWJ [19]. The delamination of the CM layers compromises its structural integrity, resulting in rejected parts, rework, and additional expenses due to material wastage and production delays. That is why avoiding CM delamination during AWJ machining is important [20,21]. When trimming, this is avoided by selecting a starting point outside the workpiece [22]. The challenge is to machine different features like holes, slots, or internal contours, where a piercing (initial material penetration) in the CM is required [21]. In aerospace, it is prohibited to pierce the CM with an AWJ [23]. Typically, holes are drilled at the starting points before engaging AWJ for further cutting, to avoid material delamination [5].

Many studies have found that the optimal combination of process parameters, including the water pressure, standoff distance, abrasive mass flow, etc., have an influence on decreasing/avoiding delamination during the piercing of CM [5,19,21]. Water pressure is particularly important as it directly influences the energy of the AWJ [19]. By employing a lower water pressure, the energy with which the AWJ impacts the CM decreases, consequently reducing the delamination [21]. The homogeneity and stability of the AWJ flow also affect delamination during piercing. Using a homogeneous AWJ and a proper combination of process parameters, CM delamination during piercing could be avoided [5]. The CM delamination phenomenon typically occurs at the beginning of the piercing process but can also manifest during AWJ cutting. In the case of the AWJ cutting process, CM delamination appears rarely. The cutting process is stable, but equipment malfunctions can create problems [24].

During the AWJ machining of composite materials, equipment malfunctions may occur, such as the following:

- The accidental reduction in the abrasive flow rate, whether partial or total, poses a significant challenge in AWJ cutting processes [19]. This reduction can occur due to various factors such as the inadvertent introduction of impurities into the abrasive delivery tank, the wear of the rubber tube used for feeding the abrasive, or the entry of water droplets into the abrasive tank. Unlike the capability to detect a complete absence of abrasive material, current AWJ equipment lacks a system capable of effectively detecting a decrease in the abrasive mass flow.
- The clogging of the cutting head with abrasive grits occurs when they partially or completely block the mixing tube [24–26]. As a result, the water jet is unable to exit through the mixing tube and may flow back up the abrasive tube, potentially reaching the abrasive hopper. This situation leads to heavy splashing, and although the cutting head moves, it fails to cut effectively.
- The orifice and focusing tube are subject to wear during abrasive waterjet machining [24,27]. The orifice is susceptible to sudden breakage, cracking, or tearing.
- A water pressure drop refers to a reduction in the force exerted by the water stream used in the AWJ process. Such a decrease can appear due to various factors, including leaks in the system, blockages in the water supply lines, or malfunctions in the pump mechanisms [26].

These malfunctions can result in CM delamination, reduced accuracy, and poor surface quality. Delamination leads to part rejection and increased expenses related to material wastage [5,9,24,27]. To avoid these issues, a real-time monitoring system may be a solution [24,27].

Acoustic Emission (AE) testing is a non-destructive evaluation (NDE) technique (EN1330-9) used to monitor and analyze the high-frequency stress waves emitted by materials under stress [28,29]. These stress waves, or acoustic emissions, occur when a material undergoes deformation, crack formation, or other structural changes. AE testing is highly sensitive and can detect the early signs of material fatigue, fractures, and other anomalies that may not be visible on the surface [30]. AE testing is widely used across various industries, including aerospace, civil engineering, manufacturing, and power generation, due to its ability to provide real-time monitoring and early warnings of potential failures [27,30,31].

AE has proven to be successful in monitoring the AWJC process [27–30]. This testing method detects and analyzes high-frequency (20 kHz–2 MHz) and low-amplitude energy waves generated during AWJC [28]. Fine changes in the AWJ process are observed in AE signal characteristics. The AE signal characteristics are also correlated with the AWJ process parameters. The AE_{RMS} and *peak-to-peak* values (*maximal amplitudes*) are dependent on the *feed rate*, particularly in the case of cutting AISI 309 material [30]. Popan et al. investigated the correlation between the AWJ cutting parameters and the AE signal and observed a correlation between the feed rate, AE_{RMS} *amplitude*, and surface quality [31].

Axinte D. et al. were able to detect cutting head clogging with abrasive particles by monitoring the *root mean square* (*RMS*) of the AE signal [24]. Kim J. et al. developed a monitoring system based on AE_{RMS} analysis to detect cutting head wear. They obtained clear patterns in the AE signal and concluded that more research is needed to develop an algorithm that automatically determines the upper and lower limits of AE_{RMS} values [27]. Amir et al. proposed and demonstrated a theory stating that the energy of the AWJ correlates and is proportional to the AE signal energy. They concluded the study by emphasizing the necessity of the mathematical modeling of AE [28].

The mathematical modeling of the AWJ process is complex due to the numerous parameters and variables involved. These models aim to predict various aspects of the AWJ process, such as material removal rate, kerf geometry, surface roughness, or jet penetration depth [32–34]. Empirical models, derived from experimental data and statistical analysis, are valuable tools for predicting the performance of the AWJ process. These models have demonstrated a good prediction accuracy, often with errors under 10%. However, a common limitation is their reliance on a relatively small number of variables [13,33]. Existing analytical models are based on fundamental principles of fluid mechanics, solid mechanics, and abrasive particle kinetics. These analytical models of AWJC also incorporate empirical correlations and experimental data to enhance their accuracy and applicability [32]. Artificial Neural Networks (ANNs) are employed to model the AWJ process, with predicted errors typically under 15% [35], demonstrating effectiveness [36].

The integration of AWJC process monitoring into the framework of digitalization and Industry 4.0/5.0 can significantly enhance operational efficiency [37], quality control, and predictive maintenance [38,39].

This paper addresses equipment malfunctions and describes the development of a monitoring method for the AWJC of composite materials. The proposed method is focused on detecting most common equipment malfunctions, including reductions or interruptions in the abrasive flow rate, the clogging of the cutting head with abrasive particles, the wear of cutting system components, and drops in the water pressure.

2. The Proposed Method for Monitoring Abrasive Waterjet Cutting

In this paper, the development of an in situ energy-based monitoring method for the Abrasive Waterjet Cutting (AWJC) of composite materials is described. The energy of the Abrasive Waterjet employed in the cutting process to erode the workpiece material is directly correlated with various process parameters such as the water pressure, feed rate, standoff distance, abrasive flow rate, and others.

The proposed method relies on the theory that the AWJ energy is closely related to Acoustic Emission (AE) signals generated during the process. By analyzing these AE signals, the method can detect anomalous events through the identification of relative variations in energy-related signals.

This monitoring technique takes into consideration both the direct jet energy involved in the erosion of the part and the jet energy lost due to friction with the cutting head. The *AE root mean square* (AE_{RMS}) values are investigated for both cases. To monitor the direct jet energy involved in the cutting (erosion) of the part, an AE sensor is mounted on the workpiece outside the cutting counter. Additionally, to monitor the jet energy lost due to friction with the internal components of the cutting head (focusing tube), another AE sensor is mounted on the cutting head. Figure 2 illustrates the proposed monitoring method.

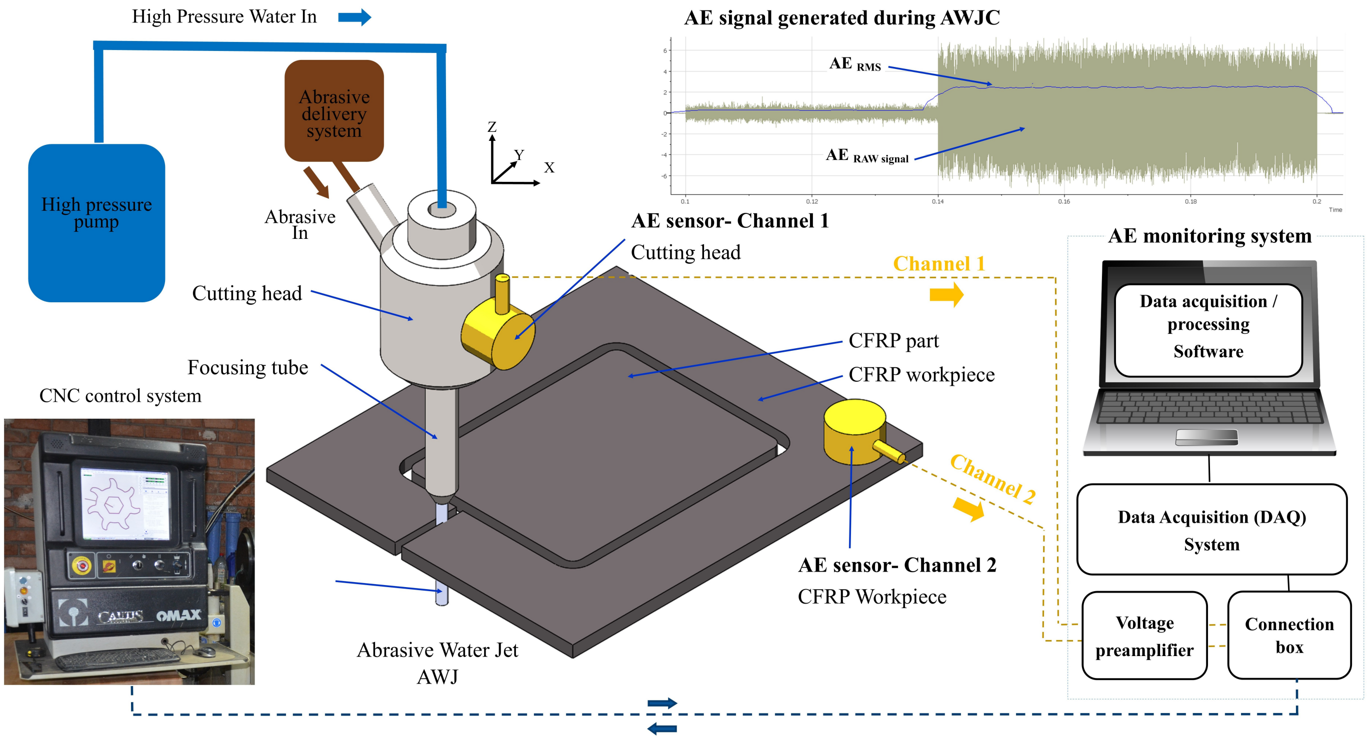

Figure 2. The proposed method for monitoring Abrasive Waterjet Cutting process.

Integrative energetic models of AWJC face challenges in establishing direct relationships between jet energies, process parameters, and process quality characteristics. The proposed method aims to empirically develop mathematical models for calculating the AE_{RMS} by considering key process parameters such as the water pressure, abrasive mass flow rate, feed rate, and material thickness. The models for AE_{RMS} offer a reference value (or the normal level) in AWJC process monitoring.

The AE monitoring technique will present the following improvements:

- Developing a smart monitoring/control system for detecting and predicting random machine malfunctions, which could damage the CM parts, also leads to a productivity and quality improvement, as well as a cost reduction.
- The variations in the AWJ energy and Acoustic Emission (AE) facilitate the verification of correct jet penetration. This ensures that the operator has selected the optimal combination of process parameters to achieve the required quality characteristics of the processed part.
- The implementation of state-of-the-art monitoring and control technologies boosts the competitiveness of companies using AWJ processing. The companies will be able to approach projects in high-end fields such as the automotive or aerospace industries, where the price of processed material is very high.

- The integration of the proposed monitoring technique within the framework of digitalization and Industry 4.0/5.0 constitutes the basis of advanced technologies and methodologies, such as Sensor Integration, Data Analytics and AI, Digital Twin Technology, Cloud Computing and Edge Computing, Integration with MES and ERP Systems, Human-Machine Interface (HMI), and Cybersecurity.

3. Materials and Methods

An experimental study was conducted to explore the correlation between the phenomena observed in AWJC and the AE signal generated during this process.

3.1. Design of Experiments

In this experimental study, Response Surface Methodology (RSM) is employed to systematically investigate the correlation between multiple independent variables and a designated response variable of interest.

The independent variables encompass water pressure, abrasive mass flow rate, feed rate, and material thickness. The output variables are represented by the *root mean square* (*RMS*) of the AE signal at the cutting head and the *RMS* of the AE signal at the workpiece.

Central Composite Design (CCD) is a frequently employed experimental design methodology in RSM. It integrates factorial points with axial points and center points, enabling the assessment of linear, quadratic, and interaction effects among factors [33]. In the context of CCD with four factors (k = 4), the total number of experimental runs is 30, comprising 16 factorial points, 8 star points, and 6 center points. The values for the independent variables and constant process parameters are presented in Table 1.

Table 1. The process parameters used in the experiment.

Process Parameters	Values
Water pressure, MPa (*P*)	100; 162.5; 225; 287.5; 350
Feed rate, mm/min (*V*)	50; 1162.5; 2275; 3387.5; 4500
Abrasive mass flow, kg/min (*Ma*)	0.1; 0.225; 0.35; 0.475; 0.6
Material thickness, mm (*t*)	1; 2; 3; 4; 5
Abrasive type and size	Garnet-mesh 80
Standoff distance, mm (*SOD*)	2
Orifice diameter, mm	0.35
Focusing tube dimensions, mm	df = 0.76/lf = 101

3.2. Equipment

During this experimental investigation, the cutting operations were conducted using the precise AWJC equipment, OMAX 2626 Jet Machining® Center. This state-of-the-art system integrates pivotal components, including a high-pressure pump, a precision CNC system, and a robust 3-axis motion system (see Figure 3a). A custom clamping system was developed for clamping the CFRP specimens, as depicted in Figure 3b.

The monitoring system developed in this research is presented in Figure 4.

The monitoring system (Figure 4b) was set up with the utilization of the PCI-6110 National Instruments data acquisition board (DAQ). This board is proficient in capturing Acoustic Emission (AE) signals at a rate of 5 million samples per second across four channels. The PCI-6110, equipped with 4 analog input ports (12-Bit, 5 MS/s/ch), 2 analog output ports, and 8 digital input–output ports. It is a simultaneous sampling, multifunction DAQ device designed for various data acquisition applications.

The AE sensors were interfaced with the analog input of the DAQ through the NI 2110 connection box, establishing a seamless connection for signal acquisition and analysis. They were seamlessly connected to the analog input of the DAQ using the NI 2110 connection box, facilitating a streamlined and efficient data acquisition process.

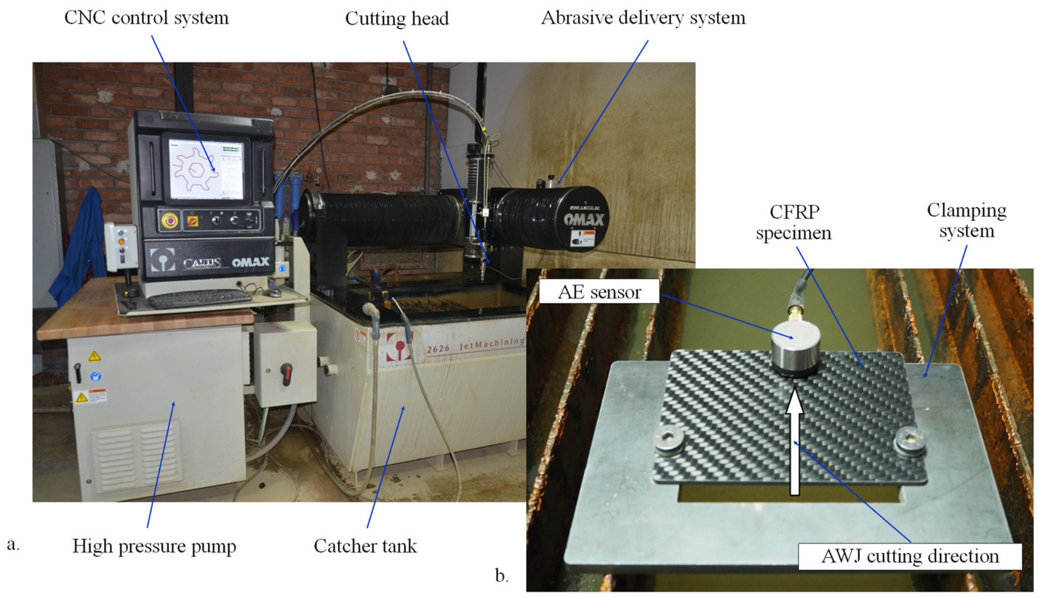

Figure 3. The experiment setup: (**a**) the Omax 2626 AWJ equipment; (**b**) the clamping system.

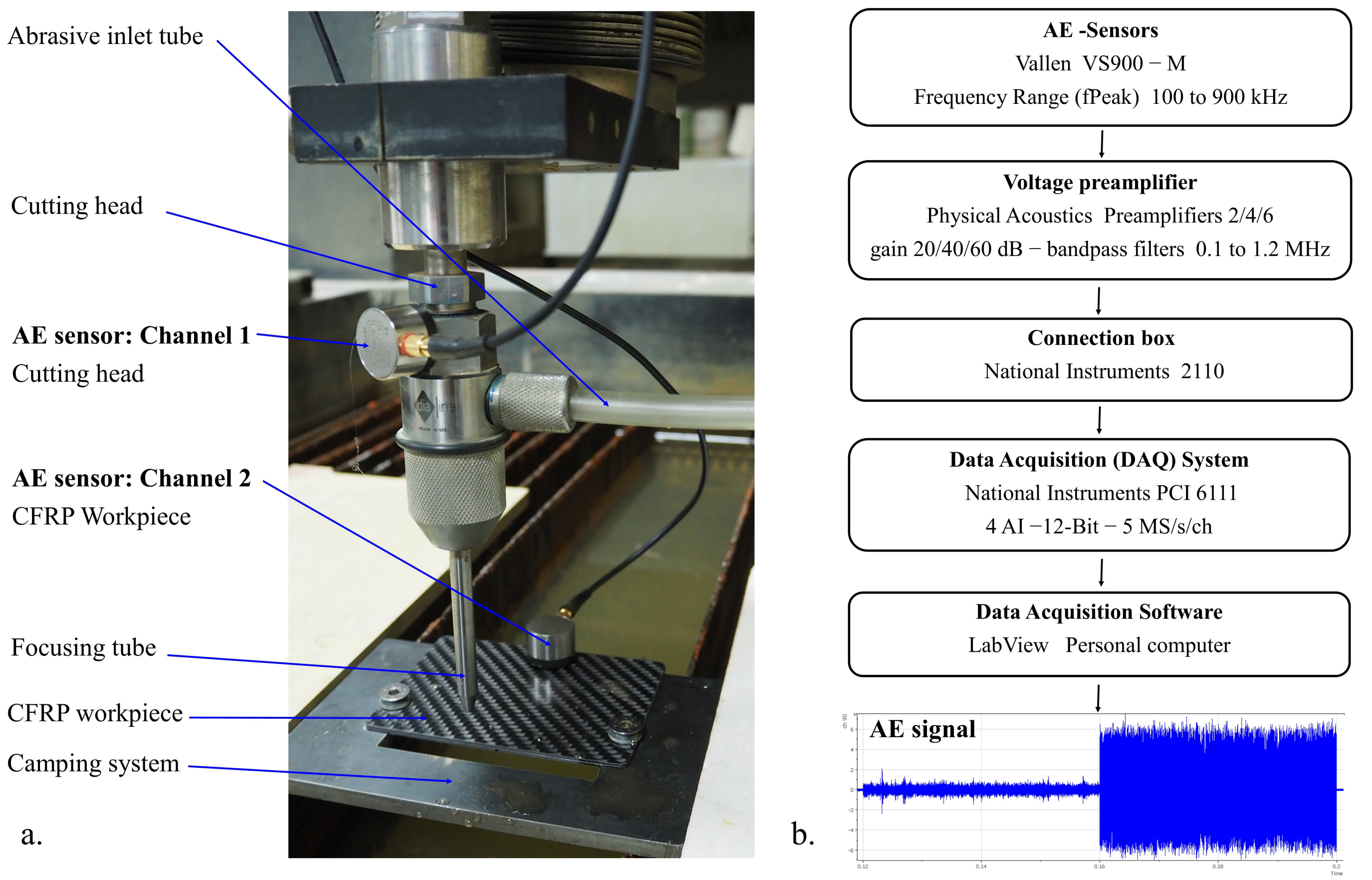

Figure 4. The AE signal acquisition setup: (**a**) the AE sensor installation, (**b**) the AE signal acquisition system architecture.

To measure Acoustic Emission, the VS900-M sensor manufactured by Vallen was employed. This passive piezoelectric AE sensor boasts a broad frequency response. The sensor features a Frequency Range (fPeak) of 100 to 900 kHz and a capacity of 540 pF. It does not come equipped with an integrated preamplifier. The sensors were glued and mechanically secured using manual clamping devices (Figure 4a).

Preamplifiers 2/4/6, provided by Physical Acoustics, were utilized to enhance the Acoustic Emission (AE) signal. Adjustable gain settings, with options of 20/40/60 dB, and internal bandpass filters covering the range of 0.1 to 1.2 MHz were incorporated. Specifically, a gain of 20 dB was chosen for signal amplification in this instance. To ensure the reliability and consistency of the results, each experiment was repeated five times.

3.3. Materials

In this experimental investigation, the chosen material is a Carbon Fiber-Reinforced Polymer (CFRP) plate sourced from ECOTEC. These CFRP sheets are manufactured using a press process in an autoclave, comprising carbon fiber prepregs with a transparent epoxy resin matrix. The non-crimp unidirectional prepreg sheet, oriented at angles of 0°/90°, possesses dimensions measuring 350 × 150 mm. Tolerances for the sheet's dimensions are specified as ±1 mm for length and width, and ±10% for thickness. The carbon fiber prepreg utilized is designated as CE 8201-200-45, characterized by a 3k fabric in style 452 in a 2/2 twill weave, and it maintains a resin content of 364 g/m^2. The sheet is designed to achieve an approximate fiber volume fraction of 60%.

The specimens under investigation were trimmed using AWJC to dimensions of 100 × 80 mm, with thicknesses ranging from 1 to 5 mm (Figure 4b).

3.4. Experimental Results

The CFRP specimens cut with an AWJ are presented in Figure 5a,b. The cut starting point was selected outside the workpiece, and the cutting length was 30 mm. The kerf generated during the cutting is plotted in Figure 5c.

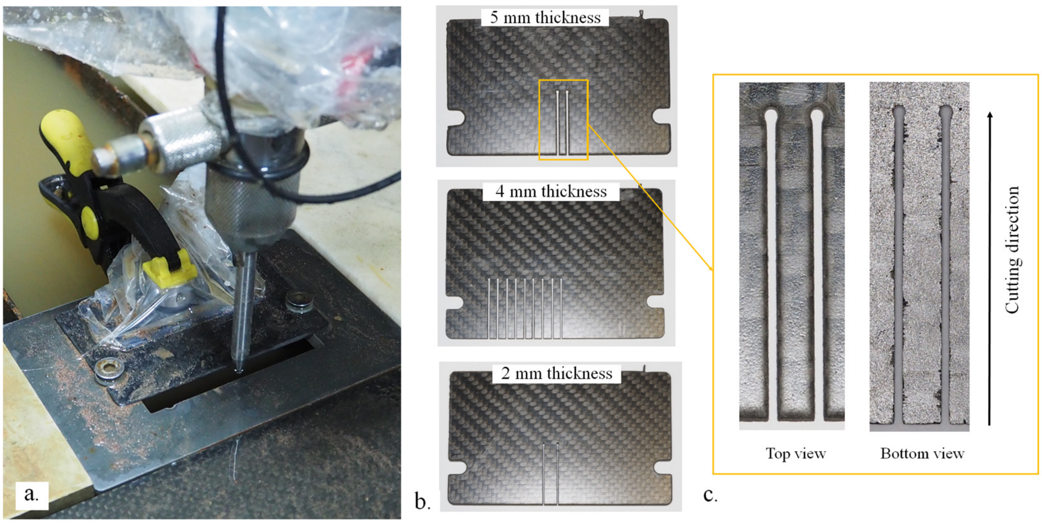

Figure 5. The CFRP cut samples during the experiment. (**a**) The experiment setup, (**b**) the cut CFRP specimens, (**c**) the generated kerf.

The *root mean square (RMS)* value of the Acoustic Emission (AE) signal was computed. The obtained values for AE_{RMS} measured at the cutting head ($AE_{RMS\ CH}$) and on the CFRP workpiece ($AE_{RMS\ WP}$) are presented in Table 2.

Table 2. The process parameters and the *root mean square (RMS)* value of the AE signal.

No.	P [MPa]	V [mm/min]	Ma [Kg/min]	T [mm]	$AE_{RMS\ CH}$ [V]	$AE_{RMS\ WP}$ [V]
1	162.5	1162.5	0.475	2	2.13	0.15
2	225	2275	0.35	3	2.75	0.1

Table 2. *Cont.*

No.	P [MPa]	V [mm/min]	Ma [Kg/min]	T [mm]	$AE_{RMS\ CH}$ [V]	$AE_{RMS\ WP}$ [V]
3	225	2275	0.1	3	1.64	1.2
4	350	2275	0.35	3	2.9	0.79
5	287.5	3387.5	0.475	4	2.85	0.6
6	225	4500	0.35	3	2.61	0.5
7	225	2275	0.6	3	2.94	0.9
8	287.5	1162.5	0.475	2	3.38	0.39
9	287.5	3387.5	0.225	4	2.53	0.94
10	287.5	1162.5	0.225	2	2.7	0.46
11	225	2275	0.35	3	2.65	0.5
12	225	2275	0.35	3	2.65	0.5
13	287.5	3387.5	0.225	2	2.72	0.62
14	225	2275	0.35	3	2.65	0.5
15	225	2275	0.35	1	2.75	0.2
16	287.5	1162.5	0.475	4	3.18	0.4
17	225	2275	0.35	3	2.65	0.5
18	287.5	1162.5	0.225	4	2.62	0.75
19	162.5	3387.5	0.225	4	1.11	0.125
20	100	2275	0.35	3	1	0.098
21	162.5	3387.5	0.475	4	1.16	0.053
22	162.5	1162.5	0.475	4	2.64	0.466
23	225	50	0.35	3	2.8	0.233
24	162.5	3387.5	0.225	2	0.67	0.056
25	162.5	3387.5	0.475	2	1.72	0.085
26	162.5	1162.5	0.225	4	1.86	0.9
27	225	2275	0.35	3	2.77	0.17
28	162.5	1162.5	0.225	2	2.18	0.32
29	287.5	3387.5	0.475	2	3.09	0.1
30	225	2275	0.35	5	2.95	0.13

4. Results and Discussion

The experimental results are utilized to explore the correlation between the phenomena occurring in AWJC and the AE signal generated during the process.

4.1. The AE Signal Analysis

The signal analysis was conducted using the NI Diadem 2023 software developed by National Instruments. Figure 6 displays the analyzed AE signal at both the cutting head and the CFRP workpiece.

The AE signal is a suitable solution for AWJC process monitoring as it provides accurate and reliable information about the changes occurring during the process.

Analyzing the AE signal acquired at the cutting head, one can clearly observe the moment the water jet starts (0.12 s), the moment when the abrasive grains are added to the WJ (0.16 s), and the moment when the AWJ stops (0.2 s). A consistent difference between the AE_{RMS} of 0.7 V for the WJ and 2.63 V measured in the case of the AWJ provides an exact moment when the abrasive is added to the WJ.

Through investigating the AE signal acquired at the CFRP workpiece, one can see the noise introduced by the AWJ before starting to cut (0.16–0.18 s), the moment when the AWJ starts cutting (0.18 s), and when the cutting finishes (0.2 s).

Through analyzing the noise introduced by the AWJ before starting the cutting (0.16–0.18 s), when the jet is positioned outside the workpiece, it can be concluded that the AE_{RMS} amplitude 0.08 V does not have an influence on the signal generated during the cutting AE_{RMS} 0.75 V.

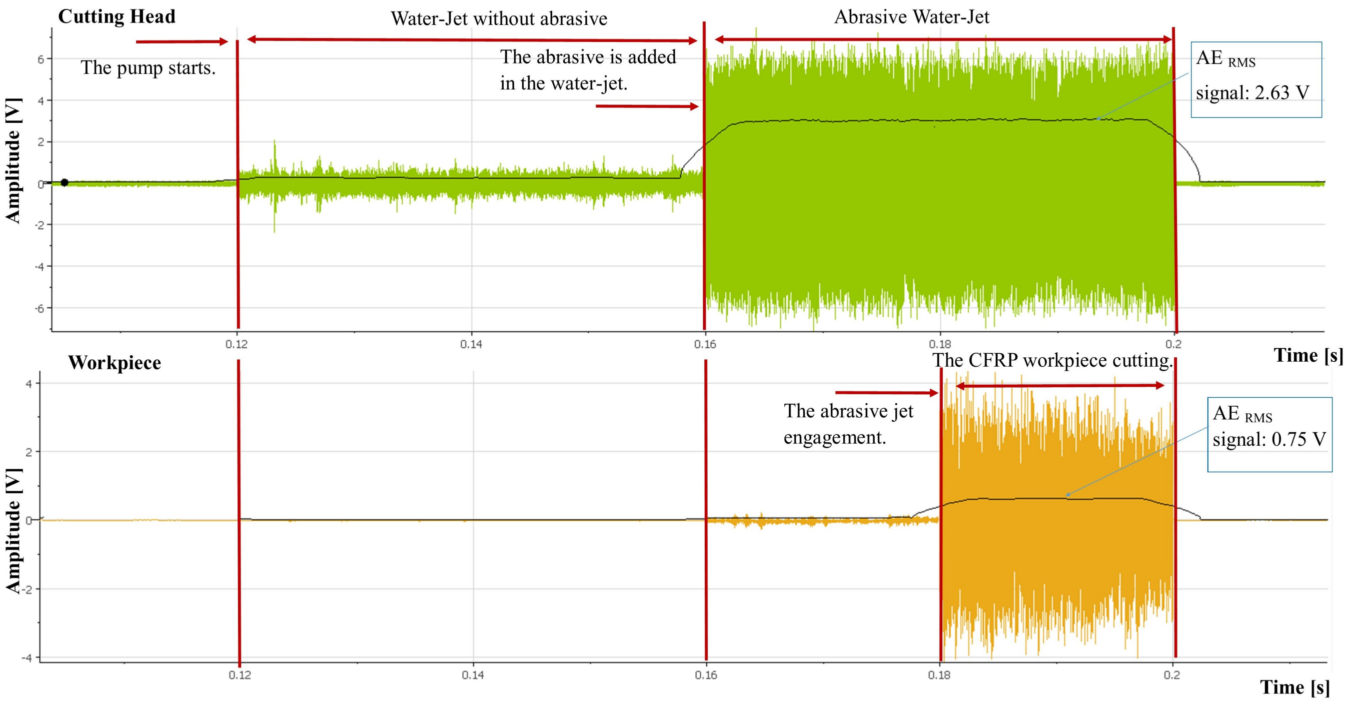

Figure 6. The main phases of the AE signal obtained during the experiment.

To extract additional insights from the signal, a frequency domain analysis was conducted. The *Fast Fourier Transform (FFT)* was employed to obtain the frequency domain, and the Hanning method was utilized to estimate the *Power Spectral Density (PSD)* of the AE signal.

The analysis of the frequency domain of the AE signal measured during the experiments revealed frequencies between 50 and 600 kHz at the cutting head (Figure 7a) and 20–400 kHz at the workpiece (Figure 7b).

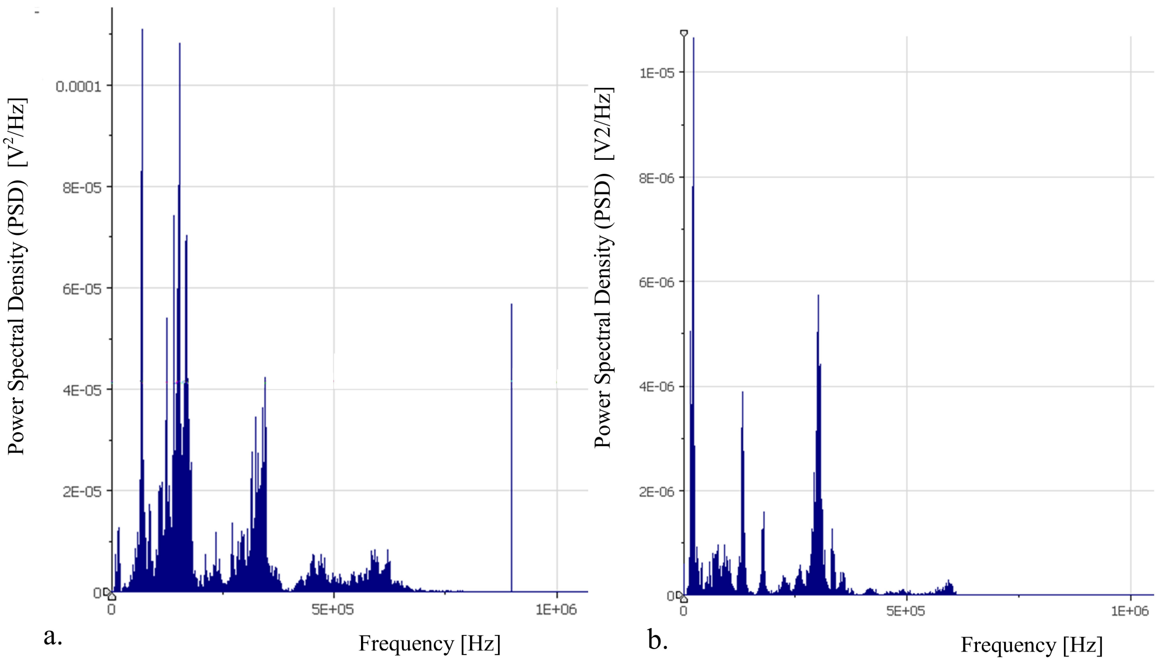

Figure 7. The frequency domain of the AE signal analyzed during the experiment (trial no. 3, P = 350 MPa, V = 2275 mm/min, Ma = 0.35 kg/min, and T = 3 mm): (**a**) the PSD of the AE signal measured at the cutting head, (**b**) the *PSD* of the AE signal measured at the CFRP workpiece.

4.2. Mathematical Modeling

The objective of this mathematical model is to obtain mathematical equations for calculating the *root mean square* of the AE signal at the cutting head ($AE_{RMS\ CH}$) and at the workpiece ($AE_{RMS\ WP}$). These mathematical models are employed to detect anomalous events in the system, providing the normal level of AE_{RMS} signal for different values of process parameters.

The chosen method for this investigation is the RSM, a set of mathematical and statistical techniques designed to articulate the connection between the response surface and independent variables (water pressure (P), abrasive mass flow rate (Ma), feed rate (V) and material thickness (T)). The analyzed models included cubic, two-factor interaction, quadratic, and linear models.

The initial dataset analyzed pertains to $AE_{RMS\ CH}$. A fitting test was conducted to assess the suitability of various models in representing the experimental data. Among these models, the quadratic model displayed a statistically significant correlation with the data (p = 0.005). This indicates a robust and meaningful representation of the relationship between the process parameters and $AE_{RMS\ CH}$. The significance level of p = 0.005 underscores the improbability of a chance occurrence, affirming the validity of the quadratic model in explaining the observed data. The statistical analysis further revealed a strong fit of the quadratic model to the data, with an *adjusted R-squared* value of 0.9168. This high *R-squared* value suggests that approximately 91% of the variability in the dependent variable can be accounted for by the model, rendering it a dependable predictor for the given dataset. The $AE_{RMS\ CH}$ model equation is provided below:

$$\begin{aligned} AE_{RMS\ CH} = 2.69 \quad & +0.56 \times P - 7.0519E - 004 \times V + 8.308 \times M_a + 0.2037 \times T \\ & +3.11011E - 006 \times P \times V + 8E - 004 \times P \times M_a - 7.8E \\ & -004 \times P \times T - 8.08909E - 005 \times V \times M_a - 2.58427E \\ & -005 \times V \times T - 0.17 \times M_a \times T - 5.41867E - 005 \times P^2 - 1.8516E \\ & -008 \times V^2 - 8.10667 \times M_a^2 + 0.01333 \times T^2 \end{aligned} \quad (1)$$

Likewise, for $AE_{RMS\ WP}$, a significant (p = 0.0001) quadratic model was fitted with an *R-squared value* of 0.883. About 88% of the variability in the dependent variable can be explained by the quadratic model. The equation of the model is

$$\begin{aligned} AE_{RMS\ WP} = 0.37 \quad & +1.7647E - 003 \times P - 4.94683E - 004 \times V - 5.19255 \times M_a \\ & +0.6777 \times T + 1.5973E - 006 \times P \times V + 5.064E - 004 \times P \times M_a \\ & +1.87E - 004 \times P \times T + 5.4382E - 005 \times V \times M_a - 1.90449E \\ & -005 \times V \times T - 0.232 \times M_a \times T - 4.136E - 006 \times P^2 + 4.4E \\ & -008 \times V^2 + 8.662 \times M_a^2 - 0.0859 \times T^2 \end{aligned} \quad (2)$$

where $AE_{RMS\ CH}$ is the *RMS* of the AE signal at the nozzle [V]; $AE_{\ RMSWP}$ is the *RMS* of the AE signal at the workpiece [V]; P is the water pressure [MPa]; Ma is the abrasive mass flow rate [kg/min]; V is the feed rate [mm/min]; and T is material thickness [mm].

To validate the regression models, 30 experimental trials were conducted. Each model was tested with 10 runs for the CFRP samples of thickness 1, 3, and 5 mm. The maximum deviation between the calculated values using the new mathematical models and the experimental values was observed to be 8.3% for $AE_{RMS\ CH}$ and 10.5% for $AE_{RMS\ WP}$.

4.3. Analysis of the Influence of Process Parameters on the AE Signal

The influence of the main AWJC process parameters on the AE signal, based on the developed mathematical models of AE_{RMS}, was analyzed.

Figure 8a illustrates the relationship between the AE_{RMS} measured at the cutting head and the process parameters. Essentially, this is the jet energy lost due to friction with the internal components of the cutting head (focusing tube). The AE_{RMS} value increases with the rise in the water pressure and abrasive mass flow rate. However, variations in the feed rate and material thickness do not affect the AE_{RMS} measured at the cutting head.

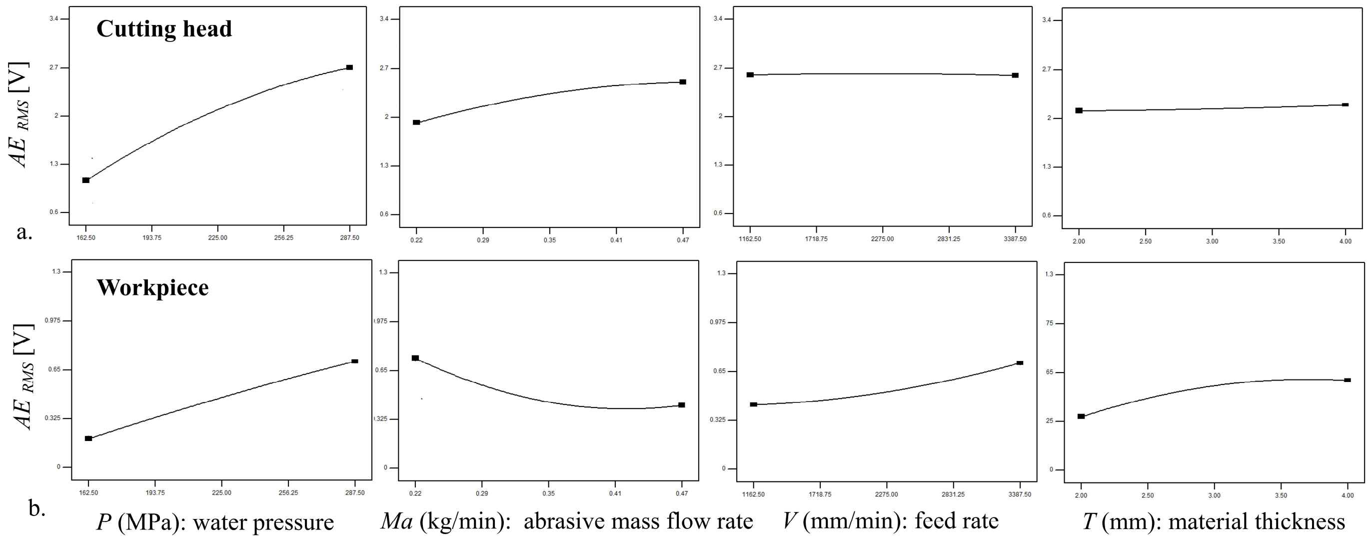

Figure 8. The influence of the process parameters on the AE signal: (**a**) the AE signal measured at the cutting head, (**b**) the AE signal measured at the CFRP workpiece.

For the AE signal measured at the CFRP workpiece, the influence of the process parameters is analyzed and presented graphically in Figure 8b. This signal is correlated with the direct jet energy involved in the cutting (erosion) of the part. Increasing the water pressure, feed rate, and material thickness results in an increase in the AE_{RMS}, while increasing the abrasive mass flow rate leads to a decrease in the value of the AE_{RMS}.

4.4. Validation of the Proposed Method for Monitoring AWJC Malfunctions

The proposed monitoring technique was validated using an experimental study. To exemplify the Acoustic Emission (AE) monitoring technique within the framework of the AWJC process, a scenario was investigated involving the accidental reduction in the abrasive flow rate.

The accidental reduction in the abrasive flow rate, whether partial or total, poses a significant challenge in AWJ cutting processes. It can lead to a compromised cutting performance and potential damage to the CFRP workpiece.

Typically, the optimal value of the abrasive flow rate is determined based on the cutting head dimensions, often through initial testing. As an example, for an Omax cutting head with an orifice diameter of 0.35 mm and focusing tube dimensions of *df* = 0.76 mm and *lf* = 101 mm, an abrasive mass flow *Ma* of 0.45 kg/min (using garnet mesh 80) is utilized.

In this case, the abrasive flow rate *Ma* decreased by approx. 50% from 0.45 kg/min to 0.23 kg/min. The AE_{RMS} signal analyzed in this scenario is plotted in Figure 9.

The initial experimental runs were conducted with an abrasive mass flow rate (*Ma*) of 0.45 kg/min. For the specified parameters (with *P* = 350 MPa, *V* = 3000 mm/min, and *T* = 4 mm), the calculated values for the AE_{RMS} at the cutting head (CH) were 3.22 V (calculated) and 3.31 V (measured), while for the workpiece (WP), they were 0.62 V (calculated) and 0.58 V (measured).

When the abrasive flow rate was reduced to 0.23 kg/min while maintaining the other operating parameters as constant, the AE_{RMS} at the cutting head (CH) was calculated to be 2.3 V, with a measured value of 2.106 V. Similarly, for the workpiece (WP), the calculated AE_{RMS} was 1.112 V, with a measured value of 1.089 V. Figure 9 presents the AE_{RMS} signals acquired during the experiments, with the AE_{RMS} obtained under decreased abrasive flow rate conditions (the malfunction) highlighted in red. In the case of the signals measured at the cutting head (Figure 9b), the AE_{RMS} value decreased from the normal value of 3.31 V (*Ma* = 0.45 kg/min) to 2.106 V (*Ma* = 0.23 kg/min) in the event of an accidental drop in the abrasive mass flow. A 48% decrease in the abrasive mass flow corresponds to a 33% decrease in the AE_{RMS}. Conversely, for the signals measured at the workpiece (Figure 9a), the AE_{RMS} value increased from the normal value of 0.58 V (Ma = 0.45 kg/min) to 1.089 V (Ma = 0.23 kg/min) under the same conditions of reduced abrasive mass flow. In this case, a decrease of 48% in the abrasive mass flow corresponds to an 87% increase in the AE_{RMS}.

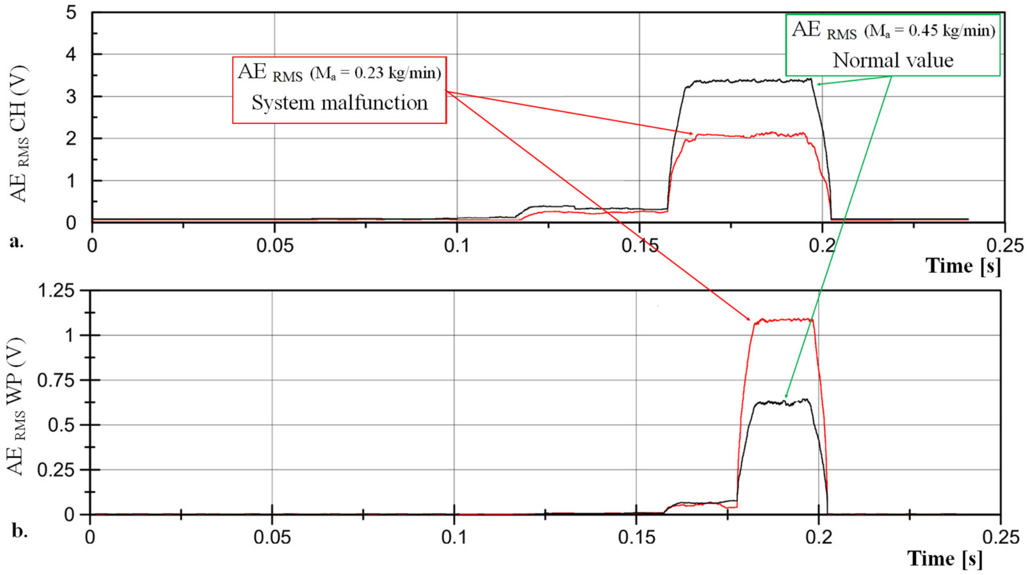

Figure 9. The AE_{RMS} signal analyzed in this scenario: (**a**) the AE signal measured at the CFRP workpiece, (**b**) the AE signal measured at the cutting head.

This equipment malfunction introduced during the AWJ cutting of CFRP results in kerf geometry modification and a decrease in the cut surface quality. Figure 10 presents the results obtained in the analyzed scenario. The dimensions of the kerf profile were measured using the PG 2000 microscope with a 9.5× zoom. The cut surface was scanned with a 3D measurement system, model µsurf Focus, and analyzed with µsoft surface analysis software.

When the equipment malfunction was introduced by reducing the abrasive flow rate from the normal value of 0.45 kg/min to 0.23 kg/min, the kerf dimensions decreased. The top kerf width (W_t) decreased from 1.33 mm to 1.26 mm, and the bottom kerf width (W_b) decreased from 0.98 mm to 0.87 mm. In the case of the cut surface topography, this malfunction resulted in an increase in the surface roughness from (R_a) 1.56 up to 2.22 µm. In the 3D topography, valleys were observed in the direction of the AWJ's movement. Additionally, the valley depth and width increased as the abrasive flow rate decreased. Similar characteristics of the surface topography were observed by Popan et al. in an investigation of the influence of AWJC process parameters on the quality characteristics of CFRP parts [40].

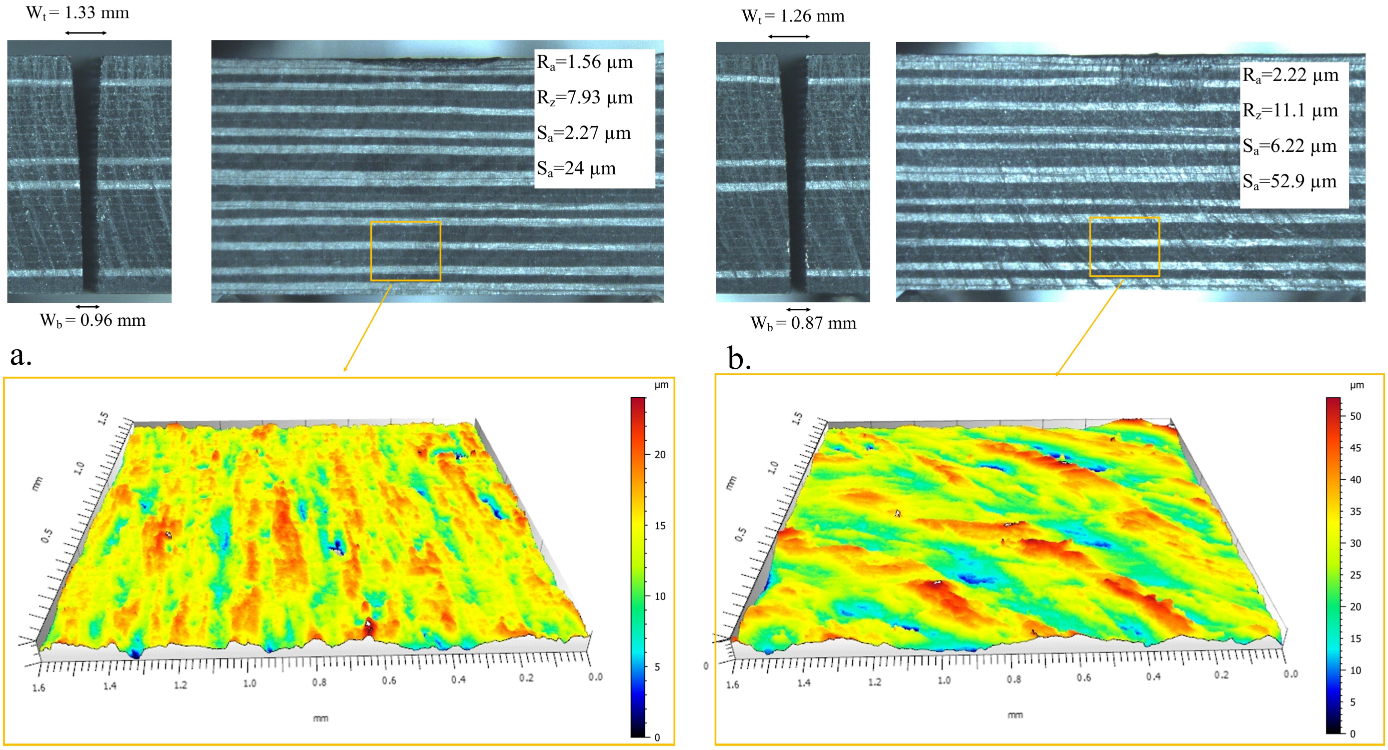

Figure 10. The kerf dimensions and the surface topography obtained in this scenario: (**a**) the normal AWJC process, (**b**) the AWJC with equipment malfunction.

5. Conclusions

This paper presents an Acoustic Emission (AE)-based monitoring method tailored for monitoring the Abrasive Waterjet Cutting process, specifically focusing on the precision processing of composite materials. Through a comprehensive experimental investigation and mathematical modeling, several key findings and contributions have emerged:

- The development of an in situ energy-based monitoring method represents a significant advancement in AWJC process monitoring. By correlating the AWJ energy with the AE signals, this method offers real-time insights into the process dynamics, enabling the detection of anomalous events and potential equipment malfunctions. Mathematical models were developed for calculating the *root mean square* of the AE signal at the cutting head and at the workpiece. These models provide a normal level of AE_{RMS} signal for different values of process parameters.
- The proposed monitoring technique enables the early detection of equipment malfunctions, such as reductions or interruptions in the abrasive flow rate, the clogging of the cutting head with abrasive particles, the wear of cutting system components, and drops in the water pressure. By promptly identifying and addressing these issues, manufacturers can minimize the risk of part rejection, material wastage, and production delays. This study examined the issue of an accidental reduction in the abrasive flow rate, outlining the pattern of this malfunction.
- The findings of this study have practical implications for industries utilizing AWJC for precision machining of composite materials. By implementing the proposed monitoring method, companies can improve the process reliability, quality assurance, and operational efficiency, ultimately enhancing the competitiveness in high-value sectors.
- Future developments in this monitoring approach could involve the integration of anomaly detection algorithms for automated fault diagnosis and process adjustment. Additionally, advancements in Industry 4.0 integration may lead to the development of smart software systems capable of real-time monitoring and analysis, further enhancing process efficiency and overall equipment effectiveness.

Author Contributions: Conceptualization, methodology, investigation: I.A.P., V.I.B., A.I.P. and C.C.; validation: I.A.P. and A.I.P.; supervision: N.B.; writing—original draft: I.A.P., V.I.B. and C.C.; research funding: N.B. All authors have read and agreed to the published version of the manuscript.

Funding: This research was supported by the HORIZON 2020—DiCoMI Project "Directional Composites through Manufacturing Innovation", GA Nr. 778068.

Institutional Review Board Statement: Not applicable.

Informed Consent Statement: Not applicable.

Data Availability Statement: The data is contained within the article.

Conflicts of Interest: The authors declare no conflicts of interest.

References

1. Poór, D.I.; Geier, N.; Pereszlai, C.; Xu, J. A Critical Review of the Drilling of CFRP Composites: Burr Formation, Characterisation and Challenges. *Compos. Part B Eng.* **2021**, *223*, 109155. [CrossRef]
2. Birleanu, C.; Pustan, M.; Pop, G.; Cioaza, M.; Popa, F.; Lazarescu, L.; Contiu, G. Experimental Investigation of the Tribological Behaviors of Carbon Fiber Reinforced Polymer Composites under Boundary Lubrication. *Polymers* **2022**, *14*, 3716. [CrossRef] [PubMed]
3. Aamir, M.; Tolouei-Rad, M.; Giasin, K.; Nosrati, A. Recent Advances in Drilling of Carbon Fiber–Reinforced Polymers for Aerospace Applications: A Review. *Int. J. Adv. Manuf. Technol.* **2019**, *105*, 2289–2308. [CrossRef]
4. Bere, P.; Neamtu, C.; Udroiu, R. Novel Method for the Manufacture of Complex CFRP Parts Using FDM-Based Molds. *Polymers* **2020**, *12*, 2220. [CrossRef]
5. Popan, I.A.; Balc, N.; Popan, A.I. Avoiding Carbon Fibre Reinforced Polymer Delamination during Abrasive Water Jet Piercing: A New Piercing Method. *Int. J. Adv. Manuf. Technol.* **2022**, *119*, 1139–1152. [CrossRef]
6. Qin, G.; Zheng, L.; Mi, P.; Zhu, Y.; Li, M.; Na, J.; Wang, Y. Influence of Single or Multi-Factor Coupling of Temperature, Humidity and Load on the Aging Failure of Adhesively Bonded CFRP/Aluminum Alloy Composite Joints for Automobile Applications. *Int. J. Adhes. Adhes.* **2023**, *123*, 103345. [CrossRef]
7. Vasile Adrian, C.; Paul, B.; Marian, B.; Sorin, G.; Cristina, B. Development of Environmental Technology for Carbon Fibre Reinforced Materials Recycling. *Mater. Plast.* **2013**, *50*, 79–83. [CrossRef]
8. Chua, C.Y.X.; Liu, H.-C.; Di Trani, N.; Susnjar, A.; Ho, J.; Scorrano, G.; Rhudy, J.; Sizovs, A.; Lolli, G.; Hernandez, N.; et al. Carbon Fiber Reinforced Polymers for Implantable Medical Devices. *Biomaterials* **2021**, *271*, 120719. [CrossRef]
9. Geier, N.; Xu, J.; Poór, D.I.; Dege, J.H.; Davim, J.P. A Review on Advanced Cutting Tools and Technologies for Edge Trimming of Carbon Fibre Reinforced Polymer (CFRP) Composites. *Compos. Part B Eng.* **2023**, *266*, 111037. [CrossRef]
10. Popan, I.A.; Cosma, C.; Popan, A.I.; Panc, N.; Filip, D.; Balc, N. Correction of Shape Error at Cut-In and Cut-Out Points in Abrasive Waterjet Cutting of Carbon Fiber Reinforced Polymer (CFRP). *Machines* **2023**, *11*, 800. [CrossRef]
11. Helmy, M.O.; El-Hofy, M.H.; El-Hofy, H. Effect of Cutting Fluid Delivery Method on Ultrasonic Assisted Edge Trimming of Multidirectional CFRP Composites at Different Machining Conditions. *Procedia CIRP* **2018**, *68*, 450–455. [CrossRef]
12. Perec, A. Experimental Research into Alternative Abrasive Material for the Abrasive Water-Jet Cutting of Titanium. *Int. J. Adv. Manuf. Technol.* **2018**, *97*, 1529–1540. [CrossRef]
13. Perec, A.; Radomska-Zalas, A.; Fajdek-Bieda, A.; Pude, F. Process optimization by applying the response surface methodology (RSM) to the abrasive suspension water jet cutting of phenolic composites. *Facta Univ.* **2022**, *21*, 575–589. [CrossRef]
14. Chen, M.; Zhang, S.; Zeng, J.; Chen, B.; Xue, J.; Ji, L. Correcting Shape Error on External Corners Caused by the Cut-in/Cut-out Process in Abrasive Water Jet Cutting. *Int. J. Adv. Manuf. Technol.* **2019**, *103*, 849–859. [CrossRef]
15. Golewski, P.; Sadowski, T.; Kneć, M.; Budka, M. The Effect of Thermal Aging Degradation of CFRP Composite on Its Mechanical Properties Using Destructive and Non-Destructive Methods and the DIC System. *Polym. Test.* **2023**, *118*, 107902. [CrossRef]
16. Mohamed, H. Trimming of CFRP Aircraft Components. In Proceedings of the 2013 WJTA-IMCA Conference and Expo, Houston, TX, USA, 9–11 September 2013.
17. Bañon, F.; Sambruno, A.; Batista, M.; Simonet, B.; Salguero, J. Study of the Surface Quality of Carbon Fiber–Reinforced Thermoplastic Matrix Composite (CFRTP) Machined by Abrasive Water Jet (AWJM). *Int. J. Adv. Manuf. Technol.* **2020**, *107*, 3299–3313. [CrossRef]
18. Chen, M.; Zhang, S.; Zeng, J.; Chen, B. Correcting Shape Error Located in Cut-in/Cut-out Region in Abrasive Water Jet Cutting Process. *Int. J. Adv. Manuf. Technol.* **2019**, *102*, 1165–1178. [CrossRef]
19. Shanmugam, D.K.; Nguyen, T.; Wang, J. A Study of Delamination on Graphite/Epoxy Composites in Abrasive Waterjet Machining. *Compos. Part A Appl. Sci. Manuf.* **2008**, *39*, 923–929. [CrossRef]
20. Dhanawade, A.; Kumar, S. Experimental Study of Delamination and Kerf Geometry of Carbon Epoxy Composite Machined by Abrasive Water Jet. *J. Compos. Mater.* **2017**, *51*, 3373–3390. [CrossRef]
21. Kim, G.; Denos, B.R.; Sterkenburg, R. Influence of Different Piercing Methods of Abrasive Waterjet on Delamination of Fiber Reinforced Composite Laminate. *Compos. Struct.* **2020**, *240*, 112065. [CrossRef]

22. Miron, A.; Balc, N.; Popan, A.; Cristina, B.; Paul, B. Studies on water jet cutting of 2D parts made from carbon fiber composite materials. *Acad. J. Manuf. Eng.* **2013**, *11*, 87.
23. Popan, A.; Cosma, C.; Popan, A.; Trif, A.; Panc, N. Abrasive water jet piercing simulation of carbon fibre reinforced polymer. *Acta Tech. Napoc.-Ser. Appl. Math. Mech. Eng.* **2023**, *66*, 209–214.
24. Axinte, D.A.; Kong, M.C. An Integrated Monitoring Method to Supervise Waterjet Machining. *CIRP Ann.* **2009**, *58*, 303–306. [CrossRef]
25. JetEdge WaterJets. Available online: https://blog.jetedgewaterjets.com/water-jet-machines/9-steps-to-prevent-water-jet-abrasive-clogs (accessed on 2 May 2024.).
26. 5 Vital Tips for Troubleshooting Your Waterjet. Available online: https://swaterjet.com/5-vital-tips-for-troubleshooting-your-waterjet (accessed on 2 May 2024).
27. Kim, J.-U.; Kim, R.-W.; Kim, S.-R.; Kim, H.-H.; Lee, K.-C. Nozzle Condition Monitoring System Using Root Mean Square of Acoustic Emissions during Abrasive Waterjet Machining. *JMMP* **2022**, *6*, 31. [CrossRef]
28. Rabani, A.; Marinescu, I.; Axinte, D. Acoustic Emission Energy Transfer Rate: A Method for Monitoring Abrasive Waterjet Milling. *Int. J. Mach. Tools Manuf.* **2012**, *61*, 80–89. [CrossRef]
29. Lissek, F.; Haeger, A.; Knoblauch, V.; Hloch, S.; Pude, F.; Kaufeld, M. Acoustic Emission for Interlaminar Toughness Testing of CFRP: Evaluation of the Crack Growth Due to Burst Analysis. *Compos. Part B Eng.* **2018**, *136*, 55–62. [CrossRef]
30. Hloch, S.; Valíček, J.; Kozak, D.; Tozan, H.; Chattopadhyaya, S.; Adamčík, P. Analysis of Acoustic Emission Emerging during Hydroabrasive Cutting and Options for Indirect Quality Control. *Int. J. Adv. Manuf. Technol.* **2013**, *66*, 45–58. [CrossRef]
31. Popan, I.A.; Bocanet, V.; Balc, N.; Popan, A.I. Investigation on Feed Rate Influence on Surface Quality in Abrasive Water Jet Cutting of Composite Materials, Monitoring Acoustic Emissions. In *Advances in Manufacturing Engineering and Materials*; Hloch, S., Klichová, D., Krolczyk, G.M., Chattopadhyaya, S., Ruppenthalová, L., Eds.; Lecture Notes in Mechanical Engineering; Springer International Publishing: Cham, Switzerland, 2019; pp. 105–113, ISBN 978-3-319-99352-2.
32. Hlaváč, L.M. Revised Model of Abrasive Water Jet Cutting for Industrial Use. *Materials* **2021**, *14*, 4032. [CrossRef] [PubMed]
33. Alexandru, P.I. Modeling and Optimization of the Abrasive Water Jet Cutting Process. In *Modeling and Optimization in Manufacturing*; Pruncu, C.I., Jiang, J., Eds.; Wiley: Oxford, UK, 2021; pp. 113–131, ISBN 978-3-527-34694-3.
34. Kong, M.C.; Anwar, S.; Billingham, J.; Axinte, D.A. Mathematical Modelling of Abrasive Waterjet Footprints for Arbitrarily Moving Jets: Part I—Single Straight Paths. *Int. J. Mach. Tools Manuf.* **2012**, *53*, 58–68. [CrossRef]
35. Grozav, S.D.; Sterca, A.D.; Kočiško, M.; Pollák, M.; Ceclan, V. Feasibility of Predictive Models for the Quality of Additive Manufactured Components Based on Artificial Neural Networks. *Machines* **2022**, *10*, 128. [CrossRef]
36. Gupta, T.V.K.; Ramkumar, J.; Tandon, P.; Vyas, N.S. Application of Artificial Neural Networks in Abrasive Water Jet Milling. *Procedia CIRP* **2015**, *37*, 225–229. [CrossRef]
37. Slavic, D.; Marjanovic, U.; Medic, N.; Simeunovic, N.; Rakic, S. The Evaluation of Industry 5.0 Concepts: Social Network Analysis Approach. *Appl. Sci.* **2024**, *14*, 1291. [CrossRef]
38. Pavlović, M.; Marjanović, U.; Rakić, S.; Tasić, N.; Lalić, B. The Big Potential of Big Data in Manufacturing: Evidence from Emerging Economies. In *Advances in Production Management Systems. Towards Smart and Digital Manufacturing*; Lalic, B., Majstorovic, V., Marjanovic, U., Von Cieminski, G., Romero, D., Eds.; IFIP Advances in Information and Communication Technology; Springer International Publishing: Cham, Switzerland, 2020; Volume 592, pp. 100–107, ISBN 978-3-030-57996-8.
39. Sofic, A.; Rakic, S.; Pezzotta, G.; Markoski, B.; Arioli, V.; Marjanovic, U. Smart and Resilient Transformation of Manufacturing Firms. *Processes* **2022**, *10*, 2674. [CrossRef]
40. Popan, I.A.; Contiu, G.; Campbell, I. Investigation on Standoff Distance Influence on Kerf Characteristics in Abrasive Water Jet Cutting of Composite Materials. *MATEC Web Conf.* **2017**, *137*, 01009. [CrossRef]